Smart Structures and Systems, Vol. 5, No. 6 (2009) 613-632
DOI: http://dx.doi.org/10.12989/sss.2009.5.6.613

Dynamic displacement tracking of a one-storey frame structure using patch actuator networks: Analytical plate solution and FE validation

Daniel Huber*

Linz Center of Mechatronics GmbH, Altenbergerstrasse 69, A-4040 Linz, Austria

Michael Krommer and Hans Irschik

Institute for Technical Mechanics, Johannes Kepler University Linz, Altenbergerstrasse 69, A-4040 Linz, Austria

(Received November 17, 2008, Accepted May 13, 2009)

Abstract. The present paper is concerned with the design of a proper patch actuator network in order to track a desired displacement of the sidewalls of a one-storey frame structure; both, for the static and the dynamic case. Weights for each patch of the actuator network found in our previous work were based on beam theory; in the present paper a refinement of these weights by modeling the sidewalls of the frame structure as thin plates is presented. For the sake of calculating the refined weights approximate solutions of the plate equations are calculated by an extended Galerkin method. The solutions based on the analytical plate model are compared with three-dimensional Finite Element results computed in the commercially available code ANSYS. The patch actuator network is put into practice by means of four piezoelectric patches attached to each of the two sidewalls of the frame structures, to which electric voltages proportional to the analytically refined patch weights are applied. Analytical and numerical results coincide very well over a broad frequency range.

Keywords: plate theory; displacement tracking; piezoelectric actuator network.

1. Introduction

Smart structure technology has become one of the key technologies for the design of modern, so-called intelligent structures in civil, mechanical and aerospace engineering. Like human beings, intelligent or smart structures react to external disturbances exerted upon them by the environment they are operating in. Over the last decades, rapid developments have been made in the modeling and control of smart structures. Crawley (1994), Tani and Tzou (1998) have presented reviews on the theory and application of smart structures and Liu, *et al.* (2005) addressed future challenges and opportunities. For practical applications of smart structures, for example in the fields of active structural vibration control as well as active noise control we refer to Alkhatib and Golnaraghi (2003), Gopinathan, *et al.* (2001), Irschik, *et al*. (2003).

The design of the smart structure is a highly multi-disciplinary task, which involves the modeling of

*Corresponding Author, E-mail: daniel.huber@lcm.at

the structure, the communication of the structure with a controller by means of suitable sensing and actuation, the integration of the smart system in the structure and the implementation of the system. One key aspect for a successful design is the communication between the structure and the controller, the so-called control-structure interaction, see Gabbert and Tzou (2001). Sensors and actuators are responsible for the functioning of this communication. In typical continuous systems a crucial point is the spatial distribution of actuators to properly perform distributed control of continua. Finding spatial actuator distributions, approximating them by discretely acting actuator networks and using them for assigning to a continuous structure an arbitrarily distributed displacement field are the main topics of the present paper.

Hence, we study the problem of how to distribute an actuation throughout a structure such that a desired displacement is exactly assigned to the structure. Such problems are denoted as dynamic displacement tracking problems. We assume the actuation to be put into practice by sources of self-stress, so-called eigenstrains; see e.g. Reissner (1931), Nemenyi (1931), Mura (1991), Irschik and Ziegler (1988). In the context of eigenstrains used as an actuation, those physical mechanisms that are exhibited by smart materials are the ones of major importance. In this latter context one often speaks about strain-induced actuation, see Tzou (1998). Although there are many such strain-induced actuation mechanisms reported in the literature (e.g. Tani, *et al.* 1998) piezoelectric actuation is the most important one for dynamic displacement tracking. Our group has been studying dynamic displacement tracking for some time; here, we refer to Irschik and Krommer (2006) and Krommer and Irschik (2007) for a three-dimensional solution and to Krommer and Varadan (2005) for thin plates.

From a practical point of view an arbitrarily distributed actuation is restricted to special cases. Once the distribution has been fixed, the applicability of the actuators to other problems is limited; patch actuator networks in contrast can be used to overcome this limitation. In the latter case the distributed nature of the actuation is approximated by the combination of a proper placement of the patch actuators and assignment of weights to the individual members of the network. The advantage of using a network is the increased flexibility in terms of design, but the disadvantage is that one can no longer find an exact solution of the dynamic displacement tracking problem.

A lot of attention has been devoted to the design of patch actuator networks (in particular using piezoelectric actuators) for the control of flexible structures. Many different strategies for the optimal placement of patch actuators are reported in the literature; see e.g. Ip and Tse (2001), Quek, *et al*. (2003), Zhang, *et al*. (2004) and Gabbert, *et al*. (2006). In most cases these strategies are based on optimization criteria related to modal and system controllability, see e.g. Sepulveda and Schmidt (1991) and Junkins and Kim (1993). As these methods are based on the projection of the dynamics of the flexible structure onto a finite-dimensional space, usually made of eigenmodes, they may not necessarily be used for dynamic displacement tracking. In the present paper the design of dense networks of actuator patches for dynamic displacement tracking constitutes the main part. The network design is based on the knowledge of the exact solution of dynamic displacement tracking by distributed actuation. Concerning our own previous research we refer to Krommer and Varadan (2006) studying dynamic shape control of sub-domains of plates by piezoelectric actuator networks and Krommer, *et al.* (2008) considering beam-type structures. For simple geometries exact analytical solutions of dynamic displacement tracking by distributed actuation can be found and for more complicated ones numerical solutions are available; e.g. for discs and shells we refer to Irschik and Pichler (2001) and Nader, *et al*. (2003). Other methods for the actuator network design, which do not use the knowledge of the exact solution for distributed actuation are based, e.g. on genetic algorithms, see Jha and Inman (2003), da Mota Silva, *et al.* (2004) and Yang, *et al*. (2005).

In the present paper we study the particular case of dynamic displacement tracking for a one-storey frame structure. In section 2 we briefly review the idea of dynamic displacement tracking of a one-storey frame structure based on modeling the structure within beam theory. First, a solution using distributed actuators is presented, which is an exact solution of the inverse problem of dynamic displacement tracking, and second, a method for the placement and weight assignment for the individual patches of a patch actuator network based on a static analysis is introduced. The results are compared to three-dimensional Finite Element computations. It turns out that (1) beam theory is not sufficient for modeling the frame structure and (2) the static weight assignment is not sufficient for higher frequencies. The problem that beam theory is not suitable is directly related to the fact that the width and the length of the sidewalls are of comparable order; hence, the kinematical assumptions of beam theory, which are, among others, based on the slenderness of beams, are no longer justified.

In section 3 we introduce a new analytical model for the frame structure, for which the frame sidewalls are modeled as thin plates, in order to get better results in comparison to the Finite Element ones. Based on this analytical model the weights assigned to the patches of the actuator network are refined for dynamic problems to overcome the limitations of the static weight assignment to the low frequency range. In this step we consider the patches to be located at the locations derived from beam theory, with the advantage that fixed locations on the one hand simplify the weight refinement and on the other hand the locations do not change for different width to length ratios of the sidewalls. In contrast, applying optimization techniques directly to the plate model with the locations and the weights not fixed a priori, would result in different locations for different width to length ratios. Such methods must be applied in case the width to length ratio no longer allows for a first approximation of the structure as a beam, but requires the consideration of plate theory from the very beginning; yet, this is not the case for the present frame structure.

Finally, numerical results are presented in section 4. The analytical model for the frame structure based on thin plate theory and the refined design for the patch actuator network are validated by means of the Finite Element computations. In both cases we find a very good agreement between analytical and numerical results, from which we conclude on the accuracy of the analytical frame model as well as on the proper patch actuator network design.

2. A short review on dynamic displacement tracking based on beam theory

In this section we shortly review the idea of dynamic displacement tracking for a one-storey frame structure based on beam theory. A laboratory setup for the structure is shown in Fig. 1(a). The ideas presented in this section have been previously published in Krommer, *et al*. (2008). Therefore, this section is not going into any detail. The novel aspect of this section in extension to our previous work is the comparison of analytical results to Finite Element computations; the discrepancy between these results motivating the rest of the present paper.

2.1. Problem formulation

We model the one-storey frame structure as a beam of length L, in which L is the height of the frame structure; a sketch of the model is also shown in Fig. 1(b). The constant bending stiffness is D and the constant linear inertia is P; the latter two entities are twice the ones of a single sidewall. The lower end of the beam is clamped and the upper end is assumed to have a zero slope. The floor, which is modeled

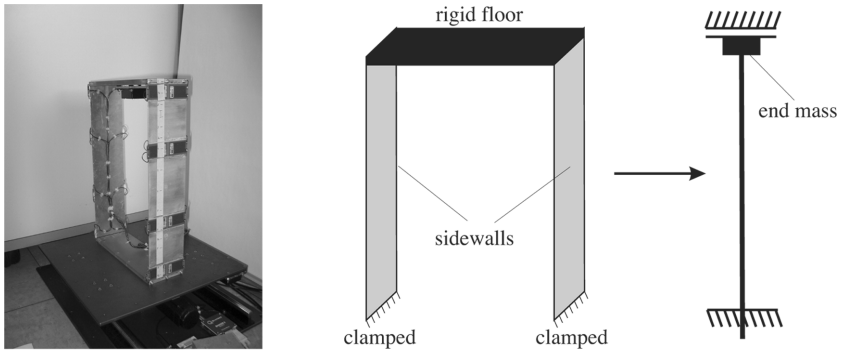

Fig. 1 One-storey frame structure: (a) laboratory setup and (b) simplified beam model

as an end mass m is assumed to only move horizontally. The only external loading of the beam is an eigenstrain type actuation $M_A(x, t)$, which we denote as actuation moment and which we use to achieve the goal of dynamic displacement tracking. As a possible actuation moment we have in mind the use of piezoelectric actuators, see also the picture in Fig. 1(a), in which piezoelectric patches are attached to the sidewalls. Yet, within this section we assume a general source of self-stress, also called an eigenstrain type actuation without further specifying its physical nature. In general, eigenstrains are incompatible strains like thermal and piezoelectric strains, but also plastic misfit strains, inclusions as well as many others, see the book by Mura (1991) for details on the notion of eigenstrains, and the original papers by Reissner (1931) and by Nemenyi (1931) for sources of self-stress (in German called "Eigenspannungsquellen"). In the case of beam theory the bending moment M_y and the actuation moment are related to each other by means of $M_y(x, t) = -Dw''(x, t) - M_A(x, t)$. $w(x, t)$ is the deflection and a prime denotes the derivative with respect to the axial coordinate x.

The actual goal of dynamic displacement tracking is to assign to both sidewalls a desired deflection, which is assumed separable with respect to the height and to time, $w_d(x, t) = w_d(x) f(t)$. We decompose the total deflection of the beam into the desired one and the deviation from the latter, $w(x, t) = w_d(x) f(t) + \Delta w(x, t)$. We can now formulate an initial-boundary value problem for the deviation of the total deflection from the desired deflection, which reads

$$
\begin{gathered}
D\frac{\partial^4 \Delta w}{\partial x^4} + P\frac{d^2 \Delta w}{dt^2} = \frac{\partial^2 M_A}{\partial x^2} - \left(D\frac{\partial^4 w_d(x)}{\partial x^4} f(t) + P w_d(x) \ddot{f}(t) \right) \\
x = 0: \Delta w = 0, \frac{\partial \Delta w}{\partial x} = 0 \\
x = L: \frac{\partial \Delta w}{\partial x} = 0, D\frac{\partial^3 \Delta w}{\partial x^3} = \frac{\partial M_A}{\partial x} - \left(D\frac{\partial^3 w_d(x)}{\partial x^3} f(t) - m w_d(x) \ddot{f}(t) \right)
\end{gathered}
\tag{1}
$$

Within his paper we assume the initial conditions trivial. The equation of motion for a beam can be found in many textbooks; here, we would like to cite only the one by Ziegler (1998).

It has been shown in our previous work (see again Krommer, *et al.* (2008) as well as Krommer and Irschik (2007)) that $\Delta w(x, t)$ is zero, if the actuation moment is assumed as $M_A(x, t) = M_1(x) f(t) - \bar{\omega}^{-2} M_2(x) \ddot{f}(t)$, with the two spatial variations as solutions of

$$\frac{\partial^2}{\partial x^2}M_1(x) = D\frac{\partial^4 w_d(x)}{\partial x^4}, \frac{\partial^2}{\partial x^2}M_2(x) = -P\overline{\omega}^2 w_d(x),$$

$$x = L: \frac{\partial M_1(x)}{\partial x} = D\frac{\partial^3 w_d(x)}{\partial x^3} \text{ and } \frac{\partial M_2(x)}{\partial x} = m\overline{\omega}^2 w_d(x). \tag{2}$$

The factor $\overline{\omega}^2$ is the square of some characteristic frequency and it is used to ensure $M_1(x)$ and $M_2(x)$ both have the dimension of a bending moment.

Dynamic displacement tracking has also been studied by Irschik and Krommer (2005, 2006) and by Krommer and Irschik (2007) for the three-dimensional case; both, with and without accounting for viscoelastic effects. Yet, these papers do not at all consider the practically important case of patch actuator networks, but rather assume the actuation to be arbitrarily distributed within the structure.

2.2. Approximate solution using actuator networks

The exact solution of the dynamic displacement tracking requires two actuation moments, both with an arbitrary time variation and spatial distribution. In practical problems it is more realistic to work with a network of n patch actuators with constant spatial variation, but with arbitrary time variations. The span of the beam is divided into n subsections $[x_i, x_i+\Delta x_i]$ with $x_1 = 0$, $x_n+\Delta x_n=L$ and $i = 1,...,n$. We assume one patch actuator is located within each subsection. The length of such an actuator is $\Delta\overline{x}_i$ and $\overline{x}_i \geq x_i$ is the location of the i-th patch satisfying the condition $\overline{x}_i + \Delta\overline{x}_i \leq x_i + \Delta x_i$. According to our previous results the locations of the patch actuators are calculated from

$$\overline{x}_i + \frac{\Delta\overline{x}_i}{2} = \left(\int_{x_i}^{x_i+\Delta x_i} M_1(x)dA\right)^{-1} \int_{x_i}^{x_i+\Delta x_i} xM_1(x)dA\,. \tag{3}$$

Furthermore, static weights are assigned to each patch actuator according to

$$M_{A1i} = \frac{1}{\Delta\overline{x}_i}\int_{x_i}^{x_i+\Delta x_i} M_1(x)dA \text{ and } M_{A2i} = \frac{1}{\Delta\overline{x}_i}\int_{x_i}^{x_i+\Delta x_i} M_2(x)dA. \tag{4}$$

Then, the actuation moment at a single patch, say the i-th patch, is considered as $M_{Ai}(t) = M_{A1i}\,f(t) - \overline{\omega}^{-2}M_{A2i}\,\ddot{f}(t)$. This design of the actuator network is based on a static analysis of the structure. In the case of static displacement tracking, in which $M_2(x)$ is not needed, the actuation as defined in Eqs. (3) and (4) will result into a deflection, which at locations x_i and L has a deflection and slope identical to the desired deflection and slope. The computation of patch locations and static weights as proposed in Eqs. (3) and (4) is again a result of our previous paper (Krommer, *et al.* 2008).

In general, applying the patch actuation moments to the frame structure, the deviation of the deflection from the desired deflection will not be zero; the error will depend on the number of patches as well as on the time variation or frequency of the desired deflection. To show this, we proceed with a numerical example.

2.3. Numerical example

As an example problem we consider the following frame structure, see the picture in Fig. 1(a). The

Table 1 Young's modulus Y and mass density ρ

Material	Y [$10^{10} Nm^{-2}$]	ρ [kgm^{-3}]
Plexiglas	70	1411
Aluminum	7.1	2684

two sidewalls are made of aluminum and the floor is made of plexiglas; as the floors are assumed rigid in the analytical model, Young's modulus of plexiglas plays no role for the analytical solution. In contrast, due to its small value it significantly affects a numerical FE solution. In order to compare the analytical solution to a numerical FE solution, we use a Young's modulus for plexiglas, which is two orders of magnitude higher than a physically realistic one in the FE model. By doing so, we ensure that the results of the present paper can be directly translated to other beam-type structures with a moderately large width compared to their length. For the future, also in the light of an experimental verification, we intend to further take the effect of the flexibility of the floor into account in the analytical model. Effective Young's modulus, which accounts for the assumption of uni-axial stress, and the mass density are given in Table 1.

The width of the sidewalls, the patch actuators as well as of the floor is $b = 0.108$ m. The sidewalls are clamped at the bottom and they are perfectly connected to each other by the floor at their upper side. The free length of the sidewalls is $L = 0.49$ m and their thickness is $h = 0.002$ m. The length of a single patch actuator is $\Delta\bar{x}_i = \Delta\bar{x} = 0.03$ m. The undistorted distance between the sidewalls is $d = 0.34$ m, which is also the horizontal length of the floor L_f. The thickness of the floor is $h_f = 0.012$ m such that its total mass becomes $m = 0.628$ kg. The bending stiffness and the linear inertia are $D = 10.224$ Nm^2 and $P = 1.1595$ kg/m. The first three beam natural frequencies are $f_1 = 5.61$ Hz, $f_2 = 46.94$ Hz, $f_3 = 124.74$ Hz.

We seek the spatial distribution of the desired deflection $w_d(x)$ to coincide with the second eigenmode of a clamped-clamped beam, see Fig. 2. In a first step we calculate the two spatial distributions of the actuation moment from Eq. (2), in which we consider the characteristic frequency to be the second natural frequency of a clamped-clamped beam with stiffness and linear inertia identical to the actual beam, $\bar{\varpi} = \omega_2^{cc}$. The result is presented in Fig. 3. Note that the solutions of Eq. (2) are not unique; any constant can be added. We have used this non-uniqueness to make the spatial distributions skew-symmetric with respect to the center of the beam axis. Next, we divide the beam into four subsections, the limits of which we choose from the zeros of $M_1(x)$. Then, we compute the locations of four patch actuators from Eq. (3). Once the locations are known, static weights are assigned to the patch actuators according to Eq. (4). The locations of the patches and the static weights are also presented in Fig. 3.

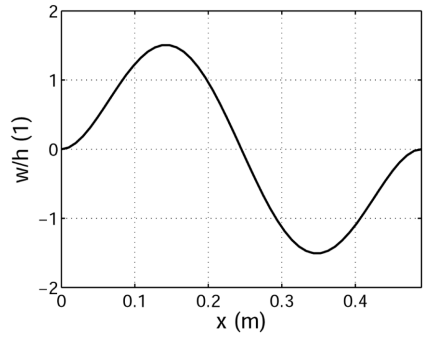

Fig. 2 Normalized second eigenmode of a clamped-clamped beam

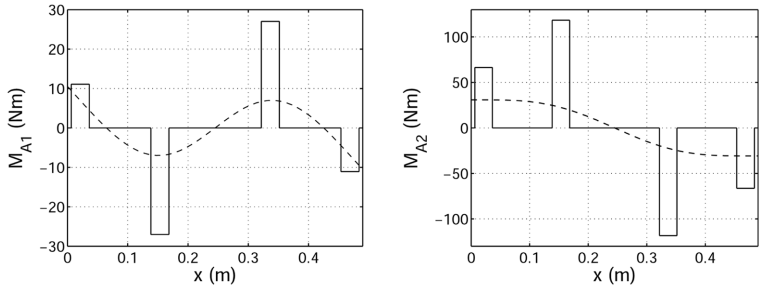

Fig. 3 Spatial distributions of the actuation moment, patch locations and static weights: (a) $M_1(x)$ and (b) $M_2(x)$

We proceed with assuming the time variation of the desired deflection to be harmonic. In this case the amplitude of the harmonic actuation moment of the patch actuators is $M_{Ai}(\omega) = M_{A1i} + (\omega/\omega_2^{cc})^2 M_{A2i}$. In the static case, $\omega = 0$, only one actuation has to applied. Besides the case $\omega = 0$, we also consider two other frequencies; namely, $f = (30,90)$Hz. These frequencies are in between the first and second natural frequency and in between the second and third natural frequency. All analytical results are compared to a harmonic analysis of the one-storey frame structure using the commercially available Finite Element code ANSYS. In the Finite Element model the patch actuators are put into practice by means of piezoelectric patches attached to both sidewalls. As our analytical solution assumes the bending stiffness and the linear inertia constant, we have used very thin piezoelectric patches ($h_p = 0.0005$ m) in the Finite Element model and we have assumed the mass density of the piezoelectric material (PZT-5A) very small. This allows for a comparison between analytical and numerical results. Details of the Finite Element model of the frame structure are given in the appendix. In order to relate the analytical actuation moment at the patches M_{Ai} to a voltage V_i to be applied to the piezoelectric patches, we have used the following formula

$$M_{Ai} = 2 \int_{z_0 = -\frac{h}{2} - h_p}^{z_1 = -\frac{h}{2}} eb \frac{V_i}{z_1 - z_0} z dz = -ebV_i(h + h_p), \tag{5}$$

in which an effective piezoelectric coefficient $e = d_{31}/S_{11} = -11.18 NV^{-1}m^{-1}$ has been considered. The factor 2 comes into the play, because we are using piezoelectric actuators at both sidewalls; hence, the total actuation moment is put into practice by two piezoelectric actuators. In Fig. 4 the results are

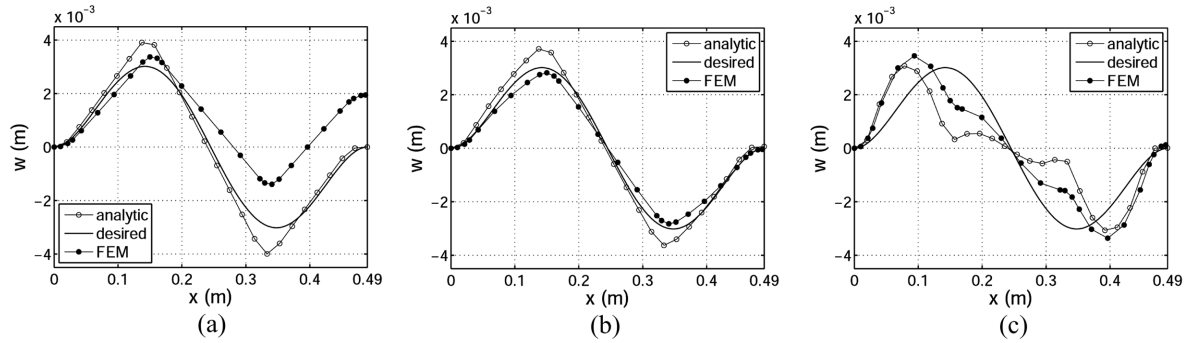

Fig. 4 Deflection amplitude: (a) $f = 0$ Hz, (b) $f = 30$ Hz and (c) $f = 90$ Hz

shown. The analytical results are identical to the ones found in (Krommer, *et al.* 2008), but the comparison to the Finite Element results was missing in our previous publication. Two conclusions must be drawn from the results. (1) The numerical results and the analytical results do not coincide at all for the static case, and (2) the goal of dynamic displacement tracking is not achieved as soon as we approach higher frequencies, not even in the analytical solution. In order to overcome these two difficulties we proceed in two directions. Firstly, we refine the assigned weights of the actuator network for higher frequencies using a method developed in (Krommer, *et al.* 2008), in which it was based on the frame structure modeled as a beam. Secondly, we update this method to the case the sidewalls are modeled as thin plates. In the latter extension to thin plates, we will derive an analytical model based on own work on analytical dynamic models for thin plates with actuator patches, see Huber, *et al.* (2008).

3. Dynamic weight and model refinement

In order to refine the weights applied to patch actuators, we assume the sidewalls of the frame structure to be modeled as thin Kirchhoff plates. We assume the domain of the rectangular plate to be $x \in [0, L]$ and $y \in [0, b]$. Each sidewall is isotropic with a plate stiffness $\overline{D}/2$ and with a linear inertia per unit area $\overline{P}/2$. If both sidewalls have the same bending motion we can model the frame structure as one plate with plate stiffness $\overline{D}$ and linear inertia $\overline{P}$. At $x = 0$ this plate is clamped and at $x = L$ the deflection is independent of y with a vanishing slope in x direction. Moreover an end mass per unit width m/b is attached to the end $x = L$. The sides of the plate at $y = 0$ and $y = b$ have to satisfy free boundary conditions. The location of the patch actuators are taken to be the ones computed within beam theory.

We assume the actuation moment at each patch is characterized by an isotropic two-dimensional second order actuation moment tensor

$$\mathbf{m}_{Ai}(t) = \mathbf{I} \sum_{j=1}^{N} m_{Aji} u_j(t) . \tag{6}$$

Here, m_{Aji} are given static weights, with $m_{A1i} = \mathrm{M}_{A1i}/b$ and $m_{A2i} = M_{A2i}/b$ known from the previous section and the remaining m_{Aji} are known, but yet to be specified; we assume the m_{Aji} to be computed from

$$m_{Aji} = \frac{1}{b\Delta x_i} \int_{x_i}^{x_i + \Delta x_i} M_j(x) dA, \; j = 1, \ldots, N, \tag{7}$$

compare Eq. (4) for $j = 1,2$. Proper choices for $M_j(x)$, $j = 3, ..., N$ will be discussed later. In contrast, the time variations $u_j(t)$ are unknown.

3.1. Dynamic weight refinement

One can easily show that the deflection $w(x, y, t)$ of the sidewalls (if assumed identical for both sidewalls) due to the actuation moment tensor can be computed from a convolution integral representation of the form:

$$\int_0^t \left[\int_0^L \int_0^b p_z^d(x, y, t - \tau) w(x, y, \tau) dy dx + \int_0^b q^d(t - \tau) w(x = L, \tau) dy \right] d\tau$$

$$= -\int_0^t \left[\sum_{i=1}^{n} \left(\sum_{j=1}^{N} m_{Aji} u_j(t-\tau) \right) \int_{\bar{x}_i}^{\bar{x}_i + \Delta\bar{x}} \int_0^b \nabla^2 w^d(x, y, \tau) dy dx \right] d\tau. \quad (8)$$

Eq. (8) represents an extension of the well-known Maysel's formula from the theory of thermal stresses to the case of general eigenstrain actuation as well as with respect to dynamics; for a comprehensive discussion of the application of Maysel's formula in the theory of thermal stresses, see Ziegler and Irschik (1987). The convolution integral in Eq. (8) has been derived in detail by Krommer and Varadan (2005, 2006). In the latter papers it was used for solving the problem of dynamic shape control of sub-domains of thin plates using piezoelectric actuators. In Krommer, *et al.* (2008) a simplified version valid for beams was used for computing refined actuator weights for the problem of dynamic displacement tracking of the frame structure based on beam theory. In the present paper we apply Eq. (8) for the computation of refined actuator weights for dynamic displacement tracking based on thin plate theory, as we have shown that beam theory is not sufficiently accurate for the present case, in which the width of the sidewalls is approximately one fifth of the length of the sidewalls.

In Eq. (8) entities with a superscript d refer to a so-called dummy loading case and ∇^2 is the two-dimensional Laplace operator. In the dummy loading case the plate is loaded by an arbitrary transverse force per unit area $p_z^d(x, y, t)$ and by a tip force per unit width $q^d(t)$, which does not depend on y; no actuation moment is applied. These dummy loadings result into the deflection $w^d(x, y, t)$.

In order to compute the unknown time variations $u_j(t)$ we have to choose $M \geq N$ dummy loading cases; we choose each of them to be applied impulsively $p_{zk}^d(x, y)\delta(t)$ and $p_z^d\delta(t)$ with $k = 1,..., M$. Hence, from the left hand side of Eq. (8) we find time functions

$$y_k(t) = \int_0^L \int_0^b p_{zk}^d(x, y) w(x, y, t) dy dx + q_k^d \int_0^b w(x = L, t) dy, \; k = 1, \ldots, M, \quad (9)$$

which we denote as sensor functions. By inserting the desired deflection into the definition of these sensor signals, we can compute the desired time variations of the sensor signals $y_{kd}(t)$ with $k = 1,...,M$. Each dummy loading case results into a dummy deflection $w_k^d(x, y, t)$, such that from Eq. (8) we have $k = 1,..., M$ coupled integral equations for the $j = 1,...,N \leq M$ unknown time variations $u_j(t)$,

$$y_{kd}(t) = -\int_0^t \left(\sum_{i=1}^{n} \left(\sum_{j=1}^{N} m_{Aji} u_j(t-\tau) \right) \int_{\bar{x}_i}^{\bar{x}_i + \Delta\bar{x}} \int_0^b \Delta w_k^d(x, y, \tau) dy dx \right) d\tau, \; k = 1, \ldots, M. \quad (10)$$

A crucial point is a proper choice of the dummy loading cases. In case $N = M$, it is near at hand to consider the spatial distribution of the dummy loadings to coincide with the spatial distribution of loadings that can be obtained from the $j = 1,\ldots, N$ functions $M_j(x)$, which are used in Eq. (7) to calculate the patch actuation. Hence, we choose the following dummy loading cases:

$$p_{zk}^d(x, y) = -\frac{1}{b} \frac{\partial^2}{\partial x^2} M_k(x), \; q_k^d = \frac{1}{b} \frac{\partial M_k(x)}{\partial x}\bigg|_{x = L}, \; k = 1, \ldots, N. \quad (11)$$

This choice results in sensor signals that are collocated to the distributed actuation moments $M_j(x)$ of Eq. (7). From a control point of view such collocation is highly desirable, see e.g. Kugi (2001), Kugi, *et al*. (2006) or Preumont (2004). In case $N < M$ additional loading cases must be chosen; this will be discussed later for our specific example problem.

In order to find a solution to the coupled integral equations, solutions for the deflection of the sidewalls of the frame structure modeled as a thin plate must be known for the dummy loading cases. As this requires the solution of partial differential equations, we will present in the next section an approximate method to derive a finite-dimensional approximation for the model of the frame structure based on thin plate theory.

3.2. A finite-dimensional model for the frame structure based on thin plate theory

In this section, we seek to derive a finite-dimensional model for the frame structure by projecting the dynamics of the frame structure onto a space made of beam eigenfunctions. Our approach considers the deflection of each of the sidewalls identical and to be approximated by the series expansion

$$w(x,y,t) \cong w^*(x,y,t) = w_1(x,y,t) + w_2(x,y,t) = \sum_{i=1}^{12} A_i(t) W_i(x,y). \tag{12}$$

In Eq. (12) the first part $w_1(x, y, t)$ considers the first eight eigenmodes of the frame structure modeled as a beam in a series expansion,

$$w_1(x,y,t) = \sum_{i=1}^{8} A_i(t) W_i(x,y), \text{ with: } W_i(x,y) = W_{xi}(x). \tag{13}$$

The eight normalized eigenmodes $W_{xi}(t)$ are shown in Fig. 5. This first part does not take any dependency of the deflection on y into account, and would therefore simply result into an approximation of the frame structure modeled as a beam. In order to incorporate the y dependency we consider the second part of the series expansion $w_2(x, y, t)$ as:

$$w_2(x,y,t) = \sum_{i=9}^{12} A_i(t) W_i(x,y), \text{ with: } W_i(x,y) = W_y(y) W_{xi}(x). \tag{14}$$

Here, the functions $W_{xi}(t)$ are taken as the first four eigenmodes of a clamped-clamped beam with a length identical to the height of the frame structure, and the function $W_y(y)$ is the first flexible free-free mode of a beam with a length identical to the width of the sidewalls. The four clamped-clamped eigenmodes and the free-free mode are shown in Fig. 6. We are using the second part of the approximation in order to account for the deviation of the deflection of the sidewalls of the frame

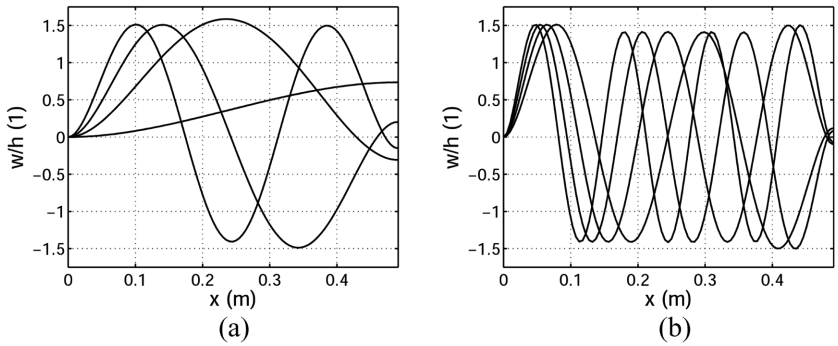

Fig. 5 First eight eigenmodes of the frame structure modeled as a beam: (a) 1-4 and (b) 5-8

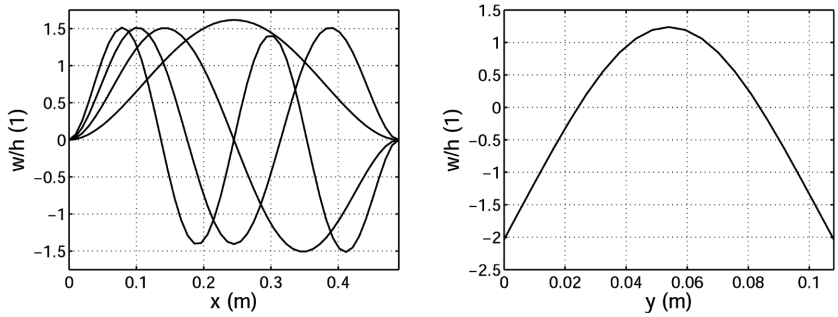

Fig. 6 (a) First four eigenmodes of a clamped-clamped beam and (b) first eigenmode of a free-free beam

structure from the deflection of a beam, as it has been obvious in the numerical results we presented so far, that beam theory is not sufficient. We would like to mention that we have already introduced this approximation for the frame structure in our previous papers, see Huber, *et al*. (2008). In extension to our previous work we have included four more eigenfunctions in the first part of the approximation in the present paper, in order to derive an analytical model of higher accuracy. This is important, because an accurate approximation is imperative for the dynamic weight refinement to work well.

With a given proper approximation for the deflection of the sidewalls we are free to choose any available method to derive a finite-dimensional dynamic model for our frame structure. Our approximation satisfies all necessary kinematical boundary conditions; yet, the dynamical boundary conditions are not satisfied. Therefore, we use an extended Galerkin procedure, in which fictitious forces and moments occur at the boundary, because the dynamical boundary conditions are not satisfied, see e.g. Ziegler (1998). The actuation due to the patch actuators is included in the fictitious boundary moments along the free boundaries as well as in additional fictitious moments at locations $\bar{x}_i$ and $\bar{x}_i+\Delta\bar{x}$, i=1,2,3,4; the extension of the Galerkin procedure with respect to eigenstrain actuation can be found in Parkus (1976), in which a thermal actuation was considered. Without going into any further details, the extended Galerkin procedure results into a finite-dimensional dynamic model of the form

$$\mathbf{M}\ddot{\mathbf{a}}(t) + \mathbf{C}\mathbf{a}(t) = \mathbf{f}(t), \tag{15}$$

in which $\mathbf{M}$ is the 12×12 mass matrix, $\mathbf{C}$ is the 12×12 stiffness matrix, $\mathbf{a}(t) = [A_1(t)\ldots A_{12}(t)]^T$ the vector of generalized coordinates and $\mathbf{f}(t) = [F_1(t)\ldots F_{12}(t)]^T$ the load vector. The mass matrix and the stiffness matrix are not diagonal, because we are using two different sets of beam eigenfunctions that are not orthogonal. The load vector accounts for a transverse force loading in the plate domain, for a tip force per unit length applied at $x = L$ and for the actuation applied at the four patch actuators.

We will use this dynamic model for the computation of the deflection in the dummy loading cases needed for the proposed method to calculate the dynamically refined patch actuator weights as well as for the simulation of the harmonically actuated frame structure.

4. Numerical example

We consider as a numerical example the frame structure we have already used before. Four patch actuators are attached to each sidewall. Yet, we consider analytical solutions to be computed by the

newly developed finite-dimensional dynamic model based on thin plate theory.

4.1. Model validation

Before we discuss dynamic displacement tracking, we validate the analytical model of the frame structure by a comparison to the Finite Element model. In Table 2 the first 6 bending natural frequencies from the analytical model are compared to the corresponding natural frequencies for open electrodes obtained from the electromechanically coupled Finite Element model; the results coincide very well.

As we have seen in the previous results the static actuator weights computed from beam theory result into an analytically computed deflection that does not at all coincide with the Finite Element solution for the static case. Therefore, we apply these static beam weights to the analytical plate model and compare the results to the Finite Element ones for the static case. The result is presented in Fig. 7; analytical and numerical results match well. Hence, the analytical plate model is much better suitable for modeling the behavior of the frame structure than the analytical beam model in the static case; for the harmonic case we will see in the next section that this is true as well. Nonetheless, the static weights are not suitable to match the desired deflection amplitude at all.

Finally, we study harmonically excited vibrations by applying to the first patch actuator (the one closest to the clamped end) a harmonic actuation moment. In Fig. 8 the absolute value of the dynamic magnification factor for the tip displacement is presented for the analytical model and the Finite Element model. The results match very well.

Table 2 First 6 bending natural frequencies of the frame structure

Natural frequency #	Analytical	Finite Element
1	5.802 Hz	5.817 Hz
2	48.63 Hz	48.80 Hz
3	129.0 Hz	130.12 Hz
4	250.2 Hz	250.09 Hz
5	412.3 Hz	411.3 Hz
6	620.6 Hz	617.4 Hz

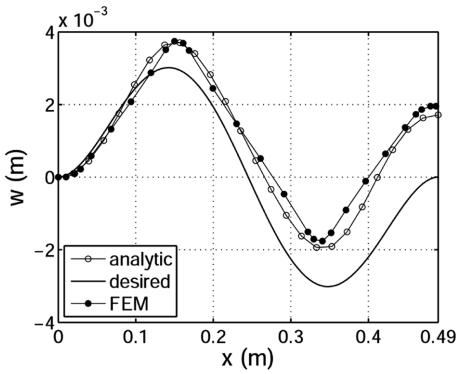

Fig. 7 Deflection amplitude for the static case using static beam weights

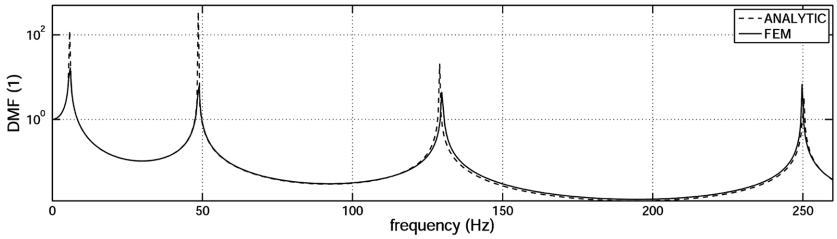

Fig. 8 Absolute value of the dynamic magnification factor for the tip displacement

4.2. Dynamic displacement tracking

In order to study the validity of our method for the computation of refined weights for dynamic displacement tracking of the frame structure we consider again harmonic displacement tracking. We use the same frame structure as in our previous example with the locations of the four patch actuators known from the actuator network design based on beam theory.

4.2.1. Actuator network design

We assume the total actuation of the network to be

$$\mathbf{m}_{Ai}(t) = \mathbf{I}\sum_{j=1}^{N} m_{Aji}U_j e^{I\omega t},\ i = 1, \ldots, 4, \tag{16}$$

see Eq. (6). The time variation is harmonic with a forcing frequency ω. The factor $e^{I\omega t}$ is understood in the following and the U_j's are the unknown amplitudes to be computed. We are using three different distributed actuators to compute the static weights for the patch actuators:

$$m_{Aji} = \frac{1}{b\Delta\bar{x}}\int_{x_i}^{x_i+\Delta x_i} M_j(x)dA,\ j = 1, \ldots, 3. \tag{17}$$

We choose static beam bending moments, which are any solution of the three incomplete simple boundary value problems:

$$\frac{\partial^2}{\partial x^2}M_1(x) = D\frac{\partial^4 w_d(x)}{\partial x^4},\ \frac{\partial^2}{\partial x^2}M_2(x) = -P(\omega_2^{cc})^2 w_d(x),\ \frac{\partial^2}{\partial x^2}M_3(x) = D\frac{\partial^4 w_4(x)}{\partial x^4},$$

$$x = L\colon \frac{\partial M_1(x)}{\partial x} = D\frac{\partial^3 w_d(x)}{\partial x^3},\ \frac{\partial M_2(x)}{\partial x} = 0,\ \frac{\partial M_3(x)}{\partial x} = D\frac{\partial^3 w_4(x)}{\partial x^3}\ . \tag{18}$$

The first two bending moments in Eq. (18) are identical to the ones shown in Fig. 3. In Eq. (18) $w_d(x)$ is the desired deflection coinciding with the second eigenmode of a clamped-clamped beam and $(\omega_2^{cc})^2$ is the square of the corresponding second natural frequency of the clamped-clamped beam. In order to get good results for higher frequencies we have included a third distributed actuation in Eq. (18), which is computed identical to the first one, but the right hand side accounts for the fourth eigenmode of the clamped-clamped beam instead of the second one. Not considering the first and third eigenmodes is motivated by the fact that our desired deflection is skew symmetric and, hence, we must not use any symmetric actuation. For a detailed discussion on the appropriateness of using these three actuators we

refer the reader to Krommer, *et al.* (2008).

4.2.2. Dummy loading cases

We choose four dummy loading cases. The first three follow directly from the bending moments of Eq. (18). We insert Eq. (18) into Eq. (11) and find

$$p_{z1}^d(x,y) = -\frac{D}{b}\lambda_2^4 w_d(x), \quad p_{z2}^d(x,y) = \frac{P}{b}\omega_2^2 w_d(x), \quad p_{z3}^d(x,y) = -\frac{D}{b}\lambda_4^4 w_4(x),$$

$$\text{with: } x = L: \quad q_1^d = \frac{D}{b}\frac{\partial^3 w_d(x)}{\partial x^3}\bigg|_{x=L}, \quad q_2^d = 0, \quad q_3^d = \frac{D}{b}\frac{\partial^3 w_4(x)}{\partial x^3}\bigg|_{x=L}. \tag{19}$$

The remaining one is introduced in order to ensure the third eigenmode of a clamped-clamped beam is not excited. Hence, we have

$$p_{z4}^d(x,y) = -\frac{D}{b}\lambda_3^4 w_3(x), \quad \text{with:} \quad x = L: \quad q_4^d = \frac{D}{b}\frac{\partial^3 w_3(x)}{\partial x^3}\bigg|_{x=L}, \tag{20}$$

in which $w_3(x)$ is the third eigenmode of the clamped-clamped beam. λ_2, λ_3 and λ_4 are eigenvalues of the clamped-clamped beam. From the four dummy loading cases we calculate four sensor signal amplitudes

$$Y_1 = \bar{Y}_1 + \bar{Y}_2, \quad Y_2 = -\bar{Y}_1, \quad Y_3 = \bar{Y}_3 + \frac{w_4'''(L)}{w_d'''(L)}\bar{Y}_2, \quad Y_4 = \bar{Y}_4 + \frac{w_3'''(L)}{w_d'''(L)}\bar{Y}_2, \tag{21}$$

in which we have introduced simpler sensor signal amplitudes

$$\bar{Y}_1 = -D\lambda_2^4 \frac{1}{b}\int_0^b\int_0^L w_d(x)w(x,y)dxdy, \quad \bar{Y}_2 = D\frac{\partial^3 w_d(x)}{\partial x^3}\bigg|_{x=L} w(x=L),$$

$$\bar{Y}_3 = -D\lambda_4^4 \frac{1}{b}\int_0^b\int_0^L w_4(x)w(x,y)dxdy, \quad \bar{Y}_4 = -D\lambda_3^4 \frac{1}{b}\int_0^b\int_0^L w_3(x)w(x,y)dxdy. \tag{22}$$

As the sensor signal amplitudes in Eq. (21) are a linear combination of the ones in Eq. (22), it is sufficient to discuss the ones in Eq. (22). Inserting the desired displacement amplitude into Eq. (22) for $w(x, y)$, one can easily obtain the desired sensor signal amplitudes, which are the sensor signal amplitudes in case the deflection is the desired one. They are:

$$\bar{Y}_{1d} = -D\lambda_2^4 \frac{1}{b}\int_0^b\int_0^L w_d(x)w_d(x)dxdy = L, \quad \bar{Y}_{id} = 0, \quad i = 2,3,4. \tag{23}$$

If our actuation were capable of ensuring these four conditions are met for the deflection it produces, we could at least conclude that (1) the expansion of the actuated deflection into a series with the second, third and fourth eigenmode of a clamped-clamped beam as base functions is identical to the desired displacement, and (2) the actuated deflection is zero at $x = L$. As our actuation is only composed of three independent actuations this will not be possible exactly, but at least in some optimal sense.

From Eq. (10) we find four linear equations for the three unknown actuator amplitudes U_j. In the harmonic case we have from Eq. (10).

$$\overline{Y}_{kd} = -\sum_{i=1}^{4}\left(\sum_{j=1}^{3} m_{Aji} U_j\right) \int_{\overline{x}_i}^{\overline{x}_i+\Delta\overline{x}} \int_{0}^{b} \nabla^2 \overline{w}_k^d(x,y)\,dy\,dx\,, \quad k = 1,...,4\,, \tag{24}$$

in which $\overline{w}_k^d(x,y)$ is the deflection due to the four dummy loading cases resulting into the sensor signal amplitudes as defined in Eq. (22). These loadings are

$$\overline{p}_{z1}^d(x,y) = -\frac{D}{b}\lambda_2^4 w_d(x)\,, \quad \overline{p}_{z2}^d(x,y) = 0\,, \quad \overline{p}_{z3}^d(x,y) = -\frac{D}{b}\lambda_4^4 w_4(x)\,, \quad \overline{p}_{z4}^d(x,y) = -\frac{D}{b}\lambda_3^4 w_3(x)\,,$$

$$\text{with: } x = L: \quad \overline{q}_1^d = 0\,, \quad \overline{q}_2^d = \frac{D}{b}\frac{\partial^3 w_d(x)}{\partial x^3}\bigg|_{x=L}\,, \quad \overline{q}_3^d = 0\,, \quad \overline{q}_4^d = 0\,. \tag{25}$$

From Eq. (24) we find a system of linear equations of the form

$$\begin{bmatrix} G_{11} & G_{12} & G_{13} \\ G_{21} & G_{22} & G_{23} \\ G_{31} & G_{32} & G_{33} \\ G_{41} & G_{42} & G_{43} \end{bmatrix} \begin{bmatrix} U_1 \\ U_2 \\ U_3 \end{bmatrix} = \begin{bmatrix} \overline{Y}_{1d} \\ 0 \\ 0 \\ 0 \end{bmatrix} \quad \leftrightarrow \quad \overleftrightarrow{G}\vec{U} = \vec{Y}\,. \tag{26}$$

We use a simple least square method to find the actuator amplitudes U_j, $\vec{U} = \left(\overleftrightarrow{G}^T \overleftrightarrow{G}\right)^{-1} \overleftrightarrow{G}^T \vec{Y}$, and moreover, the harmonic time signals to be applied to each of the four patch actuators,

$$\mathbf{m}_{Ai}(t) = \mathbf{I}\sum_{j=1}^{3} m_{Aji} U_j e^{I\omega t}\,, \quad i = 1,2,3,4\,. \tag{27}$$

The appropriateness of the design of the patch actuator network based on the four criteria given in Eq. (23) has also been investigated in detail by Krommer, *et al.* (2008) for the case of modeling the frame structure as a beam.

4.2.3. Numerical results

We consider four forcing frequencies, $\omega = 2\pi(0, 30, 90, 190)rad/s$. First we compute the actuation amplitudes U_j, $j = 1,2,3$, from which we find the individual actuation amplitudes at each patch actuator from Eq. (27). The results are presented in Table 3, in which we have also included the non-refined results obtained from beam theory (scaled with the factor $1/b$) for comparison sake. Patch 1 is the one closest to the clamped end, the weights for patch 3 are the negative weights for patch 2 and the weights for patch 4 are the negative weights for patch 1.

Finally, we present the deflection amplitudes, both for the analytical results as well as for the numerical Finite Element results, for the four forcing frequencies in Fig. 9. Note that we have used the relation given in Eq. (5) with $b = 1$ to calculate electric voltages to be applied in the Finite Element analysis. Comparing these results to the ones obtained based on beam theory, we see that the analytical results match the numerical ones much better, and that the refined actuator weights result into a displacement that is close to the desired displacement. In the static case, in which the beam solution did not work at all the results are much better; it is worth mentioning that the plate weights in this case are smaller than the beam ones. For $\omega = 2\pi 30 rad/s$ the results are comparable to the beam ones, both for the deflection amplitude as well as for the weights. For $\omega = 2\pi 90 rad/s$ we have a significant improvement, but one

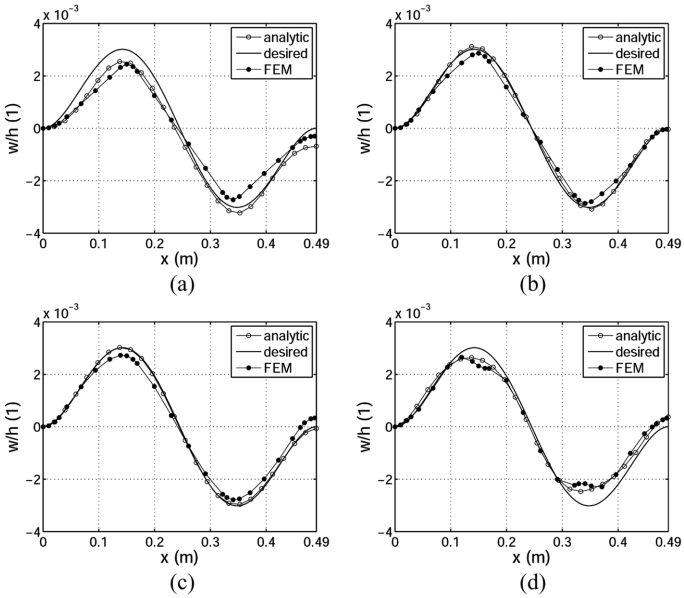

Fig. 9 Deflection amplitudes: (a) $f = 0$ Hz, (b) $f = 30$ Hz, (c) $f = 90$ Hz, (d) $f = 190$ Hz

Table 3 Individual patch actuation amplitudes [Nm/m]

f [Hz]	Patch 1		Patch 2	
	Beam	Plate	Beam	Plate
0	102.8	75.12	-250.2	-226.1
30	140.2	141.7	-183.4	-187.1
90	439.6	104.6	351.0	-73.66
190	-	-136.5	-	247.2

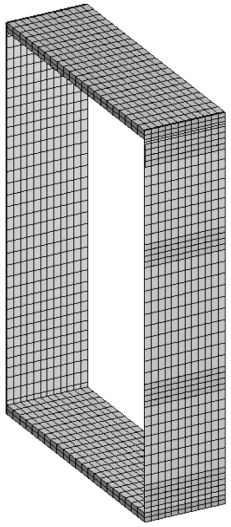

Fig. 10 Finite Element model of the frame structure

can see from Table 3 that the plate weights are much smaller than the beam ones. This clearly indicates that the beam theory is not at all suitable for the higher frequency range. In contrast, the weight refinement based on plate theory can be used up to a frequency in between the third and fourth natural frequency of the structure, $\omega = 2\pi 190 rad/s$. In order to go to higher frequencies, we would need to use more actuator patches, resulting into a denser actuator network. Yet, using only four patch actuators renders very good results over a broad frequency range.

5. Conclusions

In the present paper we have studied dynamic displacement tracking of a one-storey frame structure. Three major aspects have been discussed in detail. (1) The modeling of the frame structure as a thin plate in order to account for the relatively large width (compared to the length) of the sidewalls resulting into a significantly improved dynamic model in comparison to beam theory. (2) The computation of weights for the individual members of an actuator network constituted by patch actuators attached to the sidewalls of the frame structure in order to accurately solve the dynamic displacement tracking problem. (3) The comparison of both, the results of the dynamic analysis of the analytical plate model and of the dynamically refined actuator weights applied to the harmonic displacement tracking problem to results computed with a Finite Element model of the actual frame structure. The presented results validate the accuracy of the analytical model and the analytical solution of the tracking problem for the one-storey frame structure.

For the future we are planning on conducting research with respect to some important extensions of the method we have presented in this paper. These aspects are:

- The incorporation of domain-wise varying stiffness and linear inertia, in order to accurately model the effect of attached piezoelectric patches.
- To account for electromechanical coupling within the piezoelectric material to also properly include the sensing capabilities of piezoelectric patches.
- To generalize the method to an arbitrary and possibly high number of patch actuators constituting the actuator network; especially with respect to the choice of the spatial distribution of actuators and with respect to the proper choice of dummy loading cases.
- The extension to multi-story frame structures and to the active control of such structures by using piezoelectric patch actuator and sensor networks in combination with feedback control methods.

Besides these extensions, we are currently working on the experimental verification of the proposed method. For that sake a laboratory setup has already been constructed, see Fig. 1(a); yet, for a proper network design we still have to incorporate varying stiffness and linear inertia and the flexibility of the floor into our analytical model of the frame structure. Moreover we will have to identify effective material properties of the piezoelectric patches from the real structure to be used in the analytical solution in order to account for effects not included into the analytical plate model; among others, the bonding of the patches to the substrate structure.

Acknowledgement

Support of the authors from the Austrian Center of Competence in Mechatronics (ACCM) and of M. Krommer from the Austrian Science Fund (FWF Translational project L441-N14 “Sensor Systems for Structural and Health Monitoring”) is gratefully acknowledged.

References

Alkhatib, R. and Golnaraghi, M.F. (2003), "Active structural vibration control: a review", *Shock Vib.*, **35**(5), 367-383.

Crawley, E.F. (1994), "Intelligent structures for aerospace: a technology overview and assessment", *AIAA J.*, **32**(8), 1689-1699.

Da Mota Silva, S., Ribeiro, R., Dias Rodrigues, J., Vaz, M.A.P. and Monteiro, J.M. (2004), "The application of genetic algorithms for shape control with piezoelectric patches-an experimental comparison", *Smart Mater. Struct.*, **13**(1), 220-226.

Gabbert, U. and Tzou, H.S. (2001), *Preface: Proc. of IUTAM-Symposium on Smart Structures and Structronic Systems*, Magdeburg, Germany, September 2000.

Gabbert, U., Nestorovic-Trajkov, T. and Koppe, H. (2006), "Finite element-based overall design of controlled smart structures", *Struct. Control Health Monit.*, **13**(6), 1052-1067.

Gopinathan, S.V., Varadan, V.V. and Varadan, V.K. (2001), "Active noise control studies using the rayleigh-ritz method", *Proc. of IUTAM Symposium on Smart Structures and Structronic Systems*, September 26-29th, 2000, Magdeburg, Germany, U. Gabbert and H.S. Tzou (eds.), Solid Mechanics and its Applications, Kluwer, Dordrecht, 169-178.

Huber, D., Krommer, M. and Irschik, H. (2008), "Dynamic displacement tracking for frame structures with a piezoelectric patch network based on plate theory", *Adv. Sci. Technol.*, 56, Emboding Intelligence in Structures and Integrated Systems (*Proc. of the 3rd Int. Conf.* "*Smart Materials, Structures and Systems*", June 8-13th, 2008, Acireale, Sicily, Italy), 64-69.

Huber, D., Krommer, M. and Irschik, H. (2008), "On the influence of lateral eigenstrains on the transverse displacement of wide beams", *Proc. of the 79th Annual Meeting of the Int. Association of Applied Mathematics and Mechanics*, March 31st - April 4th, 2008, Bremen, Germany, to be published in ZAMM.

Ip, K.H. and Tse, P.C. (2001), "Optimal configuration of a piezoelectric patch for vibration control of isotropic rectangular plates", *Smart Mater. Struct.*, **10**(2), 395-403.

Irschik, H. and Krommer, M. (2005), "Dynamic displacement tracking of force-loaded linear elastic or viscoelastic bodies by eigenstrain-induced actuation stresses", *CD-Rom Proc. of IDETC/CIE 2005, ASME 2005 Int. Design Engineering Technical Conf. & Computers and Information in Engineering Conf.*, September 24-28th, 2005, Long Beach, CA, U.S.A.

Irschik, H. and Krommer, M. (2006), "Tracking of transient displacements in elastic solids and structures", *CD-Rom Proc. of 4th World Conf. on Structural Control and Monitoring (4WCSCM)*, July 11-13th, 2006, San Diego, CA, U.S.A.

Irschik, H. and Pichler, U. (2001), "Dynamic shape control of solids and structures by thermal expansion strains", *J. Therm. Stresses*, **24**, 565-578.

Irschik, H. and Ziegler, F. (1988), "Dynamics of linear elastic structures with selfstress: a unified treatment for linear and nonlinear problems", *ZAMM*, **68**, 199-205.

Irschik, H., Krommer, M., Nader, M. and Pichler, U. (2003), "Dynamic piezoelectric shape control applied of shells of revolution with translatory support excitation", *Proc. of the US - Europe Workshop on Sensors and Smart Structures Technology*, April 12-13th, 2002, Como and Somma Lombardo, Italy, L. Faravelli and B.F. Spencer, Jr., (eds.), Chichester, John Wiley & Sons, 139-148.

Jha, A.K. and Inman, D.J. (2003), "Optimal sizes and placements of piezoelectric actuators and sensors for an inflated torus", *J. Intel. Mat. Syst. Str.*, **14**(9), 563-576.

Junkins, J.L. and Kim, Y. (1993), *Introduction to Dynamics and Control of Flexible Structures*, AIAA, Washington, DC.

Krommer, M. and Irschik, H. (2007), "Sensor and actuator design for displacement control of continuous systems", *Smart Struct. Syst.*, **3**(2), 147-172.

Krommer, M. and Varadan, V.V. (2005), "Control of bending vibrations within sub - domains of thin plates - Part I: theory and exact solution", *J. Appl. Mech.*, **72**(3), 432-444.

Krommer, M. and Varadan, V.V. (2006), "Control of bending vibrations within sub - domains of thin plates - Part II: piezoelectric actuation and approximate solution", *J. Appl. Mech.*, **73**(2), 259-267.

Krommer, M., Irschik, H. and Zellhofer, M. (2008), "Design of actuator networks for dynamic displacement

tracking of beams", *Mech. Adv. Mater. Struc*., **15**(3&4), Special Issue - Design, Modelling and Experiments of Adaptive Structures and Smart Systems, 235-249.
Kugi, A. (2001), *Non - linear Control Based on Physical Models*, Springer, London.
Kugi, A., Thull, D. and Kuhnen, K. (2006), "An infinite-dimensional control concept for piezoelectric structures with complex hysteresis", *J. Struct. Control Health Monit*., **13**(6), Special Issue - Third European Conf. on Structural Control: Selected Sectional Key Note Lectures, 1099-1119.
Liu, S.C., Tomizuka, M. and Ulsoy, G. (2005), "Challenges and opportunities in the engineering of intelligent structures", *Smart Struct. Syst*., **1**(1), 1-12.
Mura, T. (1991), *Micromechanics of Defects in Solids* (2nd ed.), Kluwer, Dordrecht.
Nader, M., Pichler, U., von Garβen, H.G. and Irschik, H. (2003), "Dynamic shape control of shells of revolution by distributed piezoelectric actuation", *Proc. of of XXX Summer School APM'2002 - Advanced Problems in Mechanics*, June 27th - July 6th, 2002, St. Petersburg (Repino), Russia, A. Indeitsev, (ed.), Russian Academy of Sciences St. Petersburg, 10-17.
Nemenyi, P. (1931), "Eigenspannungen und eigenspannungsquellen", *ZAMM*, **11**, 1-8.
Parkus, H. (1976), *Thermoelasticity* (2nd ed.), Springer, Wien, New York.
Preumont, A. (2004), *Vibration Control of Active Strucutres* (2nd ed.), Kluwer, Dordrecht.
Quek, S.T., Wang, S.Y. and Ang, K.K. (2003), "Vibration control of composite plates via optimal placement of piezoelectric patches", *J. Intel. Mat. Syst. Str.*, **14**, 229-245.
Reissner, H. (1931), "Selbstspannungen elastischer Gebilde", *ZAMM*, **11**, 59-70.
Sepulveda, A.E. and Schmidt, L.A. (1991), "Optimal placement of actuators and sensors in control-augmented structural optimization", *Int. J. Numer. Meth. Eng*., **32**, 1165-1187.
Tani, J., Takagi, T. and Qiu, J. (1998), "Intelligent material systems: application of functional materials", *Appl. Mech. Rev*., **51**, 505-521.
Tzou, H.S. (1998), "Multifield transducers, devices, mechatronic systems and structronic systems with smart materials", *Shock Vib*., **30**, 282-294.
Yang, Y., Jin, Z. and Soh, C.K. (2005), "Integrated optimal design of vibration control system for smart beams using genetic algorithms", *J. Sound Vib*., **282**(3-5), 1293-1307.
Zhang, W., Qiu, J. and Tani, J. (2004), "Robust vibration control of a plate using self-sensing actuators of piezoelectric patches", *J. Intel. Mat. Syst. Str.*, **15**, 923-931.
Ziegler, F. (1998), *Mechanics of Solids and Fluids* (2nd corr. ed.), Springer, New York.
Ziegler, F. and Irschik, H. (1987), "Thermal stress analysis based on maysel's formula", *Therm. Stresses II*, R.B. Hetnarski, eds., North - Holland, Amsterdam, 120-188.

Appendix

Here, we shortly summarize the details of the Finite Element model as it was implemented in the commercially available software ANSYS[1] Workbench 11.0 SP1. The mesh is presented in Fig. 10. The total number of nodes is 16734 and the total number of elements is 2424. The two sidewalls and the floor (see Table 1 for the material parameters) are modeled using SOLID186 hexahedron elements with 20 nodes and 3 displacement degrees of freedom. The piezoelectric patches are modeled using SOLID226 elements with 20 nodes, 3 displacement degrees of freedom and one electrical voltage degree of freedom. The material parameters of the piezoelectric material (PZT-5A; polarized in the y-direction, which is normal to the plane of the sidewalls) are as follows:

- Permittivity tensor:

$$\boldsymbol{\eta} = \begin{pmatrix} \eta_{11} & 0 & 0 \\ 0 & \eta_{11} & 0 \\ 0 & 0 & \eta_{33} \end{pmatrix}, \quad \text{with} \quad \begin{cases} \eta_{11} = 1750\,\varepsilon_0 \\ \eta_{33} = 1650\,\varepsilon_0 \\ \varepsilon_0 = 8.854 \times 10^{-12}\,\text{As/Vm} \end{cases}$$

- Elasticity tensor (IEEE Standard notation):

$$\mathbf{C} = \begin{pmatrix} Q_{11} & Q_{13} & Q_{12} & 0 & 0 & 0 \\ & Q_{33} & Q_{13} & 0 & 0 & 0 \\ & & Q_{11} & 0 & 0 & 0 \\ & & & Q_{44} & 0 & 0 \\ & \text{sym.} & & & 1/2(Q_{11}-Q_{12}) & 0 \\ & & & & & Q_{44} \end{pmatrix}, \quad \text{with} \quad \begin{cases} Q_{11} = 13.9 \times 10^{10}\,\text{N/m}^2 \\ Q_{12} = 7.78 \times 10^{10}\,\text{N/m}^2 \\ Q_{13} = 7.43 \times 10^{10}\,\text{N/m}^2 \\ Q_{33} = 11.5 \times 10^{10}\,\text{N/m}^2 \\ Q_{44} = 2.56 \times 10^{10}\,\text{N/m}^2 \end{cases}$$

- Tensor of piezoelectric moduli:

$$\mathbf{e} = \begin{pmatrix} 0 & e_{31} & 0 \\ 0 & e_{33} & 0 \\ 0 & e_{31} & 0 \\ 0 & 0 & e_{15} \\ 0 & 0 & 0 \\ e_{15} & 0 & 0 \end{pmatrix}, \quad \text{with} \quad \begin{cases} e_{31} = -5.2\,\text{C/m}^2 \\ e_{33} = 15.1\,\text{C/m}^2 \\ e_{15} = 12.7\,\text{C/m}^2 \end{cases}$$

[1]ANSYS, Inc.; www.ansys.com